REPTATION QUANTUM MONTE CARLO

a round-trip tour from classical diffusion to quantum mechanics

STEFANO BARONI* AND SAVERIO MORONI†
SISSA – Scuola Internazionale Superiore di Studi Avanzati,
INFM – Istituto Nazionale per la Fisica della Materia,
via Beirut 2-4, 34014 Trieste Grignano, Italy

Abstract. We present an elementary and self-contained account of the analogies existing between classical diffusion and the imaginary-time evolution of quantum systems. These analogies are used to develop a new quantum simulation method which allows the calculation of the ground-state expectation values of local observables without any mixed estimates nor population-control bias, as well as static and dynamic (in imaginary time) response functions. This method, which we name *Reptation Quantum Monte Carlo* , is demonstrated with a few case applications to ^{4}He, including the calculation of total and potential energies, static and imaginary-time dependent density response functions, and low-lying excitation energies. Finally, we discuss the relations of our technique with other simulation schemes.

1. Introduction

The theory of stochatic processes plays an important role in modern developments of quantum mechanics both as a deep—and possibly not yet fully exploited—conceptual method [1, 2] and as a powerful practical tool for the computer simulation of interacting quantum systems [3]. Quantum Monte Carlo simulations mainly rely on the *static* properties of a random walk of one kind or another that is used to sample the ground-state wave-function or finite-temperature density matrix of a system. Comparatively minor attention has been paid so far to the *dynamical* properties of the random walks used in quantum simulations. The main interest in these properties stems from the study of excitation energies, a notoriously difficult and ill-conditioned problem. These dynamical properties, also determine the magnitude of autocorrelation times which are necessary to estimate statistical errors.

The purpose of these lectures is to provide an elementary and self-contained presentation of the deep relations existing between diffusion in classical systems and the imaginary-time evolution of quantum systems, and to develop some ideas based on these relations [4] which lead to a new, promising technique for performing quantum simulations. For reasons which will become apparent in the following, we name this technique *Reptation Quantum Monte Carlo* (RQMC). The main features of RQMC are that it is based on a *purely diffusive* process without branching, that ground-state expectation values of local observables can be evaluated without any mixed estimates, and that static and dynamic (in imaginary time) response functions are natural by-products of the ground-state simulation. Although some of the ideas presented here are not new [4], our method does not suffer from the drawbacks which affected their previous implementations.

2. From classical diffusion to quantum mechanics

The simplest phenomenological description of classical diffusion is given by the Langevin equation:

$$dx = f(x)d\tau + d\xi, \tag{1}$$

where x is some generalized coordinate describing our system, $f(x) = -\frac{\partial v(x)}{\partial x}$ is the force acting on it—which we suppose to be derivable from a potential—τ is time and $\xi(\tau)$ is a Wiener process: $\langle d\xi \rangle = 0$; $\langle (d\xi)^2 \rangle = 2d\tau$. Although the random walk generated by the Langevin equation, Eq. (1), can be given a mathematically unambiguous meaning in the continuous limit, it is simpler—and more useful in view of applications to quantum simulations—to specialize to a given discretization of time: $\tau_k = k \times \epsilon$. The corresponding random walk is then described by the discrete Markov chain:

$$x_{k+1} = x_k + \epsilon f(x_k) + \xi_k, \tag{2}$$

where the ξ's are uncorrelated Gaussian random variables of zero mean, $\langle \xi_i \rangle = 0$, and variance 2ϵ, $\langle \xi_i \xi_j \rangle = 2\epsilon\delta_{ij}$.

2.1. THE FOKKER-PLANCK EQUATION

The time evolution of the probability distribution for the variable x is given by the master equation which, in the one-dimensional case, reads (the generalization to many dimensions is straightforward):

$$P(x, \tau + \epsilon) = \int \mathcal{W}_\epsilon(x|y) P(y, \tau)\, dy, \tag{3}$$

where

$$\mathcal{W}_\epsilon(x|y) = \frac{1}{\sqrt{4\pi\epsilon}} \mathrm{e}^{-\frac{(x-y-\epsilon f(y))^2}{4\epsilon}} \tag{4}$$

is the conditional probability that the system is in configuration x at time $\tau + \epsilon$, given that it is found in configuration y at time τ. When the conditional probability is independent of τ (as it is in the present case) the corresponding Markov process is said to be *homogeneous*. In order to convert the master equation, Eq. (3), into a differential equation, we perform a Taylor expansion of its right-hand side in powers of the time step ϵ:

$$P(x, \tau + \epsilon) = \frac{1}{\sqrt{4\pi\epsilon}} \int \delta(x - y - \epsilon f(y) - \xi) \mathrm{e}^{-\frac{\xi^2}{4\epsilon}} P(y, \tau)\ d\xi\ dy. \tag{5}$$

Taking into account that $\xi \sim \sqrt{\epsilon}$, we now formally Taylor-expand the δ function in powers of $(\epsilon f(y) + \xi)$, and we obtain:

$$P(x, \tau + \epsilon) = \int P(y, \tau) \left(\sum_n \frac{(-1)^n}{n!}\ \delta^{(n)}(x - y) \times \langle (\epsilon f(y) + \xi)^n \rangle \right)\ dy, \tag{6}$$

where $\langle \cdot \rangle$ indicates the Gaussian average of the polynomials in ξ, and $\delta^{(n)}$ is the n-th derivative of the δ function:

$$\begin{aligned} \langle (\epsilon f(y) + \xi)^n \rangle &\equiv \frac{1}{\sqrt{4\pi\epsilon}} \int_{-\infty}^{\infty} (\epsilon f(y) + \xi)^n \mathrm{e}^{-\frac{\xi^2}{4\epsilon}} d\xi \\ &= (-i\sqrt{\epsilon})^n H_n \left(i \frac{\sqrt{\epsilon}}{2} f(y) \right), \end{aligned} \tag{7}$$

H_n being the Hermite polynomial of order n [5]. To linear order in ϵ, the first few values of these Gaussian integrals are: $\langle \epsilon f(y) + \xi \rangle = \epsilon f(y)$, $\langle (\epsilon f(y) + \xi)^2 \rangle = 2\epsilon + \mathcal{O}\left(\epsilon^2\right)$, $\langle (\epsilon f(y) + \xi)^3 \rangle = \mathcal{O}\left(\epsilon^2\right)$. Integrals of the derivatives of the δ function are given by: $\int g(y) \delta^{(n)}(x - y)\ dy = g^{(n)}(x)$. Using this relation, Eq. (6) can be recast as:

$$P(x, \tau + \epsilon) = P(x, \tau) + \epsilon \left(-\frac{\partial}{\partial x} \Big(f(x) P(x, \tau) \Big) + \frac{\partial^2 P(x, \tau)}{\partial x^2} \right) + \mathcal{O}\left(\epsilon^2\right). \tag{8}$$

Eq. (8) is the discrete-time version of the Fokker-Planck equation which, in the continuous limit, reads [6]:

$$\frac{\partial P(x, \tau)}{\partial \tau} = \frac{\partial^2 P(x, \tau)}{\partial x^2} - \frac{\partial}{\partial x} \Big(f(x) P(x, \tau) \Big). \tag{9}$$

The fact that this equation is first order in time is strictly related to the Markovian character of the random walk, Eq. (2). It is easily verified that

$P_s(x) \propto \mathrm{e}^{-v(x)}$ is a stationary solution of the Fokker-Planck equation, Eq. (9). Using Eq. (8) one sees that the stationary distribution of the *discrete* random walk, Eq. (2), differs from P_s by terms of order ϵ.

The conditional probability, $\mathcal{W}_\epsilon$, defined in Eq. (4), can be seen as the *exact* probability that the system described by the *discrete* Markov chain, Eq. (2), makes a transition from configuration y to configuration x during the time step ϵ; alternatively, it can be seen as an approximation to the transition probability in the continuous limit, correct to order $\mathcal{O}(\epsilon^2)$. In the continuous limit the exact conditional probability is defined by the relation:

$$P(x,\tau) = \int \mathcal{W}(x,\tau|y,0)P(y,0)dy. \tag{10}$$

By inserting this definition into Eq. (9), one sees that $\mathcal{W}(x,\tau|y,0)$ satisfies Eq. (9) with respect to x, subject to the boundary condition: $\mathcal{W}(x,0|y,0) = \delta(x-y)$, *i.e.* $\mathcal{W}(x,\tau|y,0)$ is the Green's function of the Fokker-Planck equation, Eq. (9). The Markovian character of random walk, Eq. (2), allows one to define a simple functional-integral representation for $\mathcal{W}(x,\tau|y,0)$ [7] which closely resembles the path-integral representation of the Green's function of the time-dependent Schrödinger equation [8]. As we will see in the following, this resemblance is by no means accidental nor superficial.

Let $X_N = \{x_0, x_1, \cdots, x_N\}$ be a given random walk generated by Eq. (2). Because of the Markovian character of the chain, the corresponding probability density, $\boldsymbol{\mathcal{P}}_\epsilon[X_N]$ satisfies the relation:

$$\begin{aligned}
\boldsymbol{\mathcal{P}}_\epsilon[X_N] &\equiv \mathtt{Prob}[x(N\epsilon) = x_N; x((N-1)\epsilon) = x_{N-1}; \cdots; x(0) = x_0] \\
&= \mathcal{W}_\epsilon(x_N|x_{N-1})\mathtt{Prob}[x((N-1)\epsilon) = x_{N-1}; \cdots; x(0) = x_0] \\
&= \mathcal{W}_\epsilon(x_N|x_{N-1})\boldsymbol{\mathcal{P}}_\epsilon[X_{N-1}],
\end{aligned} \tag{11}$$

where $x(\tau)$ is the configuration of the system at time τ. By iterating this equation N times, one obtains:

$$\boldsymbol{\mathcal{P}}_\epsilon[X_N] = \mathcal{W}_\epsilon(x_N|x_{N-1})\mathcal{W}_\epsilon(x_{N-1}|x_{N-2})\cdots\mathcal{W}_\epsilon(x_1|x_0)P(x_0,0). \tag{12}$$

The probability density that the system is in configuration x_N at time $\tau = N\epsilon$ is obtained from $\boldsymbol{\mathcal{P}}_\epsilon[X_N]$ by integrating out the N variables, $\{x_0, \cdots, x_{N-1}\}$:

$$\begin{aligned}
P(x_N, N\epsilon) &= \int \boldsymbol{\mathcal{P}}_\epsilon[\{x_0, \cdots, x_N\}]dx_0 \cdots dx_{N-1} \qquad (13) \\
&= \int \mathcal{W}_\epsilon(x_N|x_{N-1})\cdots\mathcal{W}_\epsilon(x_1|x_0)P(x_0,0)dx_0\cdots dx_{N-1}.
\end{aligned}$$

By comparing Eq. (10) with Eq. (13), one obtains the desired functional-integral representation for $\mathcal{W}$:

$$\begin{aligned}\mathcal{W}(x,\tau|y,0) &= \\ &\int \mathcal{W}_\epsilon(x|x_{N-1})\mathcal{W}_\epsilon(x_{N-1}|x_{N-2})\cdots\mathcal{W}_\epsilon(x_1|y)\ dx_1\cdots dx_{N-1} = \\ &(4\pi\epsilon)^{-\frac{N}{2}}\int \mathrm{e}^{-\frac{1}{4\epsilon}\sum_{k=0}^{N-1}(x_{k+1}-x_k--\epsilon f(x_k))^2}dx_1\cdots dx_{N-1},\end{aligned} \tag{14}$$

where $\epsilon = \tau/N$, $x_0 = y$, and $x_N = x$. The above representation is *exact* for the *discrete* Markov chain described by Eq. (2). In the continuous limit ($\epsilon \to 0$) it is understood that it holds by letting $N = \tau/\epsilon \to \infty$, while keeping τ fixed.

2.2. THE CLASSICAL-QUANTUM MAPPING

In order to establish the link between classical diffusion and imaginary-time quantum evolution, we define a wave-function, $\Phi(x,\tau)$, through the relation:

$$P(x,\tau) = \Phi_0(x)\Phi(x,\tau), \tag{15}$$

where $\Phi_0(x) = \sqrt{P_s(x)} \propto \mathrm{e}^{-v(x)/2}$. By inserting Eq. (15) into Eq. (8) and dividing by $\Phi_0(x)$, we obtain:

$$\Phi(x,\tau+\epsilon) = (1-\epsilon\mathcal{H})\ \Phi(x,\tau) + \mathcal{O}\left(\epsilon^2\right), \tag{16}$$

where:

$$\mathcal{H} = -\frac{\partial^2}{\partial x^2} + \mathcal{V}(x), \tag{17}$$

and

$$\begin{aligned}\mathcal{V}(x) &= \frac{1}{4}\left(\frac{\partial v}{\partial x}\right)^2 - \frac{1}{2}\,\frac{\partial^2 v}{\partial x^2} \\ &= \frac{1}{\Phi_0(x)}\frac{\partial^2\Phi_0(x)}{\partial x^2}\ .\end{aligned} \tag{18}$$

The continuous-time limit of Eq. (16) is formally equivalent to an imaginary-time Schrödinger equation,

$$\frac{\partial\Phi(x,\tau)}{\partial\tau} = -\mathcal{H}\ \Phi(x,\tau), \tag{19}$$

which could as well have been derived directly by inserting Eq. (15) into Eq. (9).

The wave-function Φ_0 is a solution of Eq. (19), which means that it is an eigenfunction of the time-independent Schrödinger equation, corresponding to a zero eigenvalue. A general theorem of quantum mechanics states that the ground-state eigenfunction of a Schrödinger equation with a local potential is non-degenerate and node-less [9]. Orthogonality with respect to excited-state wave-functions implies that the ground state is the only node-less eigenfunction. We thus arrive at the conclusion that all the excited-state energies are strictly positive and that $\Phi_0(x)$ is the only time-independent solution of Eq. (19) or, equivalently, that $P_s(x) \propto \mathrm{e}^{-v(x)}$ is the only stationary solution of the Fokker-Planck equation (9) [10]. Furthermore, any solution of Eq. (9) would tend to P_s for large times, irrespective of the initial condition. If the spectrum of $\mathcal{H}$ has a gap, the approach to equilibrium is exponentially fast. This is easily seen by simple inspection. Consider a system whose probability distribution at time $\tau = 0$ is $P(x,0)$ and its expression in terms of the eigenfunctions and eigenvalues of $\mathcal{H}$, which we indicate by Φ_n and $\mathcal{E}_n$:

$$P(x,0) = \Phi_0(x) \sum_n c_n \Phi_n(x). \tag{20}$$

The time evolution of P is readily derived from the time evolution of the Φ's:

$$P(x,\tau) = c_0 \Phi_0(x)^2 + \sum_{n \neq 0} c_n \mathrm{e}^{-\mathcal{E}_n \tau} \Phi_0(x) \Phi_n(x). \tag{21}$$

The normalization of $P(x,0)$ and the orthonormality of the Φ's imply that $c_0 = 1$ and that the norm of $P(x,\tau)$ is conserved. The above equation shows that the thermalization time—*i.e.* the time necessary for the system to reach equilibrium—is $\tau_0 \approx \frac{1}{\mathcal{E}_1}$.

The fact that P_s is the only stationary solution of the Fokker-Planck equation, Eq. (9), implies that classical expectation values over P_s—or, equivalently, quantum expectation values over $\Phi_0(x)$—can be expressed as time averages over the random walk, $x(\tau)$, generated by the Langevin equation, Eq. (1):

$$\int P_s(x) \mathcal{A}(x)\ dx \equiv \langle \Phi_0 | \mathcal{A} | \Phi_0 \rangle = \lim_{T \to \infty} \lim_{t \to \infty} \frac{1}{t} \int_T^{T+t} \mathcal{A}\left(x(\tau)\right)\ d\tau. \tag{22}$$

A comparison between Eq. (3) and Eq. (16) allows one to establish a relation between the transition probability of the classical random walk, $\mathcal{W}_\epsilon$, and the propagator of the quantum system associated with it:

$$\mathcal{W}_\epsilon(x|y) = \Phi_0(x) \mathcal{G}(x,y;\epsilon) / \Phi_0(y) + \mathcal{O}\left(\epsilon^2\right), \tag{23}$$

where:

$$\mathcal{G}(x,y;\tau) \equiv \langle x | \mathrm{e}^{-\tau \mathcal{H}} | y \rangle. \tag{24}$$

The fact that the error in Eq. (23) is indeed of second order in ϵ, and not higher, can be proved by pushing the Taylor expansion of Eq. (6) to second order in ϵ and by noting, for instance, that the second-order term would give rise to a non-hermitian contribution to $\mathcal{G}$. Using Eqs. (12) and (23), the probability density for the random walk X_N can be easily expressed in terms of a product of quantum propagators, $\mathcal{G}$. Assuming that the system is at equilibrium at $\tau = 0$—*i.e.* that the probability distribution for x_0 is $P_s(x_0)$—the probability distribution for the random walk is:

$$\begin{aligned} \boldsymbol{\mathcal{P}}_\epsilon[X_N] &= \underbrace{\Phi_0(x_N)\mathcal{G}(x_N, x_{N-1};\epsilon)\cdots\mathcal{G}(x_1, x_0;\epsilon)\Phi_0(x_0)}_{\boldsymbol{\mathcal{P}}[X_N]} + \mathcal{O}\left(\epsilon\right) \\ &\equiv \boldsymbol{\mathcal{P}}[X] \times \boldsymbol{\mathcal{Q}}_\epsilon[X_N], \end{aligned} \tag{25}$$

where $\boldsymbol{\mathcal{Q}}_\epsilon[X_N] = 1 + \mathcal{O}\left(\epsilon\right)$ is a time-discretization correction factor. The Markovian character of the random walk implies a simple composition law for the $\boldsymbol{\mathcal{P}}$ probability distributions:

$$\begin{aligned} \boldsymbol{\mathcal{P}}[\{x_0, \cdots, x_k, \cdots, x_N\}] = \boldsymbol{\mathcal{P}}[\{x_0, \cdots, x_k\}]\times \\ \boldsymbol{\mathcal{P}}[\{x_k, \cdots, x_N\}]/P_s(x_k). \end{aligned} \tag{26}$$

Inspection of Eq. (25) shows that the probability distribution $\boldsymbol{\mathcal{P}}[X]$ is invariant under time reversal:

$$\boldsymbol{\mathcal{P}}[\bar{X}] = \boldsymbol{\mathcal{P}}[X], \tag{27}$$

where $\bar{X} \equiv \{x_N, \cdots, x_0\}$ is the path obtained from X under time reversal. In the short-time limit, this time-reversal invariance simply expresses the detailed balance condition:

$$\mathcal{W}_\epsilon(x|y)P_s(y) \approx \mathcal{W}_\epsilon(y|x)P_s(x). \tag{28}$$

As it can be seen from Eq. (23), the above relation holds to $\mathcal{O}\left(\epsilon^2\right)$, and from a mathematical point of view it is strictly connected with the hermitian character of the quantum propagator, $\mathcal{G}$.

2.3. CLASSICAL VS. QUANTUM TIME CORRELATION FUNCTIONS

Eq. (22) expresses the identity between classical thermal expectation values of local observables and quantum expectation values of the same observables calculated over the ground state of a suitably defined auxiliary system. Furthermore, these expectation values can be expressed in terms of time averages over a random walk. In the following we will see how this result can be extended to time correlation functions. It will result that (real) time correlation functions calculated over the random walk coincide with the ground-state imaginary-time correlation functions of the auxiliary quantum system.

The time auto-correlation function of an observable $\mathcal{A}(x)$ is defined as:

$$\langle \mathcal{A}(\tau)\mathcal{A}(0)\rangle = \int \mathcal{A}(x)\mathcal{A}(y)\ \mathtt{Prob}[x(0)=y; x(\tau)=x]\ dxdy. \qquad (29)$$

If the stochastic process is stationary (*i.e.* if $P(x,\tau) = P_s(x)$), then one has:

$$\begin{aligned} \mathtt{Prob}[x(0)=y; x(\tau)=x] &= \mathcal{W}(x,\tau|y,0)P_s(y) \\ &= \Phi_0(x)\mathcal{G}(x,y;\tau)\Phi_0(y). \end{aligned} \qquad (30)$$

By inserting this relation into Eq. (29), the auto-correlation function reads:

$$\begin{aligned} \langle \mathcal{A}(\tau)\mathcal{A}(0)\rangle &= \int \mathcal{A}(x)\mathcal{A}(y)\Phi_0(x)\mathcal{G}(x,y;\tau)\Phi_0(y)dxdy \\ &= \langle \Phi_0|\mathrm{e}^{\mathcal{H}\tau}\mathcal{A}\mathrm{e}^{-\mathcal{H}\tau}\mathcal{A}|\Phi_0\rangle \\ &\equiv \langle \Phi_0|\mathcal{A}(-i\tau)\mathcal{A}(0)|\Phi_0\rangle, \end{aligned} \qquad (31)$$

where we have used the fact that $\mathrm{e}^{\mathcal{H}\tau}|\Phi_0\rangle = |\Phi_0\rangle$ and the definition of a time-dependent operator in the Heisenberg representation: $\mathcal{A}(t) = \mathrm{e}^{i\mathcal{H}t}\mathcal{A}\ \mathrm{e}^{-i\mathcal{H}t}$.

Eq. (31) can be used to express the autocorrelation time of the observable $\mathcal{A}$ in terms of the spectral properties of the auxiliary quantum Hamiltonian, $\mathcal{H}$. The autocorrelation time is defined as the time integral of the normalized autocorrelation function:

$$\tau_{\mathcal{A}} = \int_0^\infty \underbrace{\frac{\langle \mathcal{A}(\tau)\mathcal{A}(0)\rangle - \langle \mathcal{A}\rangle^2}{\langle \mathcal{A}^2\rangle - \langle \mathcal{A}\rangle^2}}_{c_{\mathcal{A}}(\tau)} d\tau. \qquad (32)$$

The integrand in Eq. (32) is defined in such a way that $c_{\mathcal{A}}(0) = 1$ and $c_{\mathcal{A}}(\infty) = 0$. When $c_{\mathcal{A}}$ is exponential, $\tau_{\mathcal{A}}$ is simply its decay constant: $c_{\mathcal{A}}(\tau) = \mathrm{e}^{-\tau/\tau_{\mathcal{A}}}$. In practical simulations, $\tau_{\mathcal{A}}$ determines the statistical errors in the measure of $\mathcal{A}$:

$$\langle \mathcal{A}\rangle \approx \frac{1}{N}\sum_{i=M+1}^{M+N} \mathcal{A}(x_i) \pm \sqrt{\Delta\mathcal{A}^2\frac{\tau_{\mathcal{A}}}{N\epsilon}}, \qquad (33)$$

where M is chosen large enough so that equilibrium is reached (*i.e.* $M > \frac{1}{\epsilon E_1}$), and $\Delta\mathcal{A}^2 \approx \frac{1}{N-1}\sum(\mathcal{A}(x_i) - \langle\mathcal{A}\rangle)^2$. In order to proceed further, we first consider the spectral resolution of the quantum propagator, $\mathcal{G}$:

$$\mathcal{G}(x,y;\tau) = \sum_n \mathrm{e}^{-\mathcal{E}_n\tau}\Phi_n(x)\Phi_n(y). \qquad (34)$$

By inserting Eq. (34) into Eq. (31), the auto-correlation time can be easily cast into the form:

$$\tau_{\mathcal{A}} = \frac{1}{\Delta\mathcal{A}^2}\sum_{n\neq 0}\frac{|\langle\Phi_n|\mathcal{A}|\Phi_0\rangle|^2}{\mathcal{E}_n}. \tag{35}$$

3. From quantum mechanics back to classical diffusion

The purpose of many quantum simulation techniques is to study the ground-state properties of a system whose Hamiltonian is

$$H = -\frac{\partial^2}{\partial x^2} + V(x), \tag{36}$$

and whose (unknown) ground-state wave-function and energy we indicate by Ψ_0 and E_0, respectively. In the variational Monte Carlo method (VMC), an approximate wave-function, Φ_0, is used to generate a random walk according to the discrete Langevin equation, Eq. (2), with

$$\begin{aligned} f(x) \equiv f_{VMC}(x) &= -\frac{\partial}{\partial x}\left(-\log\Phi_0(x)^2\right) \\ &= 2\frac{1}{\Phi_0(x)}\frac{\partial\Phi_0(x)}{\partial x}, \end{aligned} \tag{37}$$

and the ground-state expectation value of the operator $\mathcal{A}$ is estimated through Eq. (33), where $\mathcal{A}(x) = \frac{1}{\Phi_0(x)}\mathcal{A}\Phi_0(x)$. Systematic errors in Eq. (33) depend on the discretization of time and are of order ϵ. They can be eliminated in principle by enforcing the detailed-balance condition on the master equation, Eq. (3) [11]. A variational upper bound, $\bar{\mathcal{E}}$, to the ground-state energy can be estimated from Eq. (33):

$$\bar{\mathcal{E}} \equiv \langle\Phi_0|H|\Phi_0\rangle \approx \frac{1}{N}\sum_i \mathcal{E}(x_i), \tag{38}$$

where

$$\mathcal{E}(x) = \frac{1}{\Phi_0(x)}H\Phi_0(x) \tag{39}$$

is the so-called *local energy*. In the following we will show how the *dynamical* properties of the random walk (1) can be used to systematically improve upon this VMC procedure and to estimate, *exactly* within statistical noise, the ground-state properties of quantum systems.

Let us first observe that the trial wave-function, Φ_0, implicitly defines a reference (unperturbed) Hamiltonian, H_0, whose *exact* ground state is Φ_0.

The potential function which defines H_0 is simply obtained by inverting the time-independent Schrödinger equation:

$$V_0(x) = \frac{1}{\Phi_0(x)} \frac{\partial^2 \Phi_0(x)}{\partial x^2} + \bar{\mathcal{E}}. \tag{40}$$

A comparison between Eq. (40) and Eqs. (17,18) shows that the potential obtained from the inversion of the Schrödinger equation coincides up to a constant with the effective quantum potential resulting from the classical-quantum mapping discussed in Sec. 2.2 ($V_0(x) = \mathcal{V}(x) + \bar{\mathcal{E}}$), provided that the classical random walk, Eqs. (1,2), is driven by the VMC force defined in Eq. (37).

The original Hamiltonian, Eq. (36), can then be cast into the form:

$$H = \underbrace{-\frac{\partial^2}{\partial x^2} + \mathcal{V}(x)}_{\mathcal{H}} + \bar{\mathcal{E}} + \underbrace{\mathcal{E}(x) - \bar{\mathcal{E}}}_{\Delta\mathcal{H}}. \tag{41}$$

By construction, Φ_0 is the ground state of $\mathcal{H}$, and $\mathcal{E}(x) = E_0$ if Φ_0 is the ground state of H. When Φ_0 is not the ground state of H, the local energy $\mathcal{E}(x)$ is not a constant, and the ground-state properties of H can in principle be obtained by perturbation theory with respect to $\Delta\mathcal{H}$.

Let us calculate the corrections to the ground-state energy, E_0, up to second order in $\Delta\mathcal{H}$. The first-order correction vanishes by construction, given that $\langle\Phi_0|H|\Phi_0\rangle = \bar{\mathcal{E}}$. The second-order correction is given by:

$$\Delta E_0^{(2)} = -\sum_{n\neq 0} \frac{|\langle\Phi_0|\mathcal{E}|\Phi_n\rangle|^2}{\mathcal{E}_n}, \tag{42}$$

where $\mathcal{E}$ is the local energy *operator*, and we have taken into account the fact that the unperturbed ground-state energy is zero ($\mathcal{E}_0 = 0$). By comparing this expression with Eq. (35), the second-order correction to the ground-state energy can be expressed in terms of the fluctuations of the local energy and of its auto-correlation time:

$$\Delta E_0^{(2)} = -\tau_{\mathcal{E}} \Delta\mathcal{E}^2. \tag{43}$$

In the following, we show how this relation between perturbative corrections to the ground-state energy and (integrals of) auto-correlation functions of the local energy along the random walk can be generalized to arbitrary order. The resulting perturbation series can be effectively summed to infinite order by an appropriate re-sampling of the random walks generated by the VMC Langevin equation, Eqs. (1,2,37).

3.1. STOCHASTIC PERTURBATION THEORY

Given the Hamiltonian H, Eq. (36), and a trial wave-function, Φ_0, which we suppose to be non-orthogonal to its ground state, Ψ_0, the ground-state energy of H can be expressed as:

$$E_0 = \lim_{\tau\to\infty} \frac{\langle\Phi_0|H\mathrm{e}^{-H\tau}|\Phi_0\rangle}{\langle\Phi_0|\mathrm{e}^{-H\tau}|\Phi_0\rangle} = -\lim_{\tau\to\infty}\frac{d}{d\tau}\log\langle\Phi_0|\mathrm{e}^{-H\tau}|\Phi_0\rangle \tag{44}$$

$$= -\lim_{\tau\to\infty}\frac{1}{\tau}\log\langle\Phi_0|\mathrm{e}^{-H\tau}|\Phi_0\rangle. \tag{45}$$

These equations are easily demonstrated by expressing Φ_0 as a linear combination of the eigenfunctions of H, $\{\Psi_n\}$: $\Phi_0 = \sum_n c_n\Psi_n$, and by inserting this expression into Eqs. (44,45):

$$\log\langle\Phi_0|\mathrm{e}^{-H\tau}|\Phi_0\rangle = -E_0\tau + \log\left(c_0^2\right) + \mathcal{O}\left(\mathrm{e}^{-(E_1-E_0)\tau}\right). \tag{46}$$

The following basic identity holds:

$$\mathcal{Z}_0 \equiv \langle\Phi_0|\mathrm{e}^{-H\tau}|\Phi_0\rangle = \int \mathrm{e}^{-\boldsymbol{\mathcal{S}}[X]}\boldsymbol{\mathcal{P}}[X]\,\boldsymbol{\mathcal{D}}[X]$$

$$\equiv \left\langle \mathrm{e}^{-\boldsymbol{\mathcal{S}}[X]}\right\rangle, \tag{47}$$

where $\boldsymbol{\mathcal{P}}[X]$ is the probability distribution for the random walk X, Eq. (25), $\boldsymbol{\mathcal{D}}[X] = dx_0\cdots dx_N$, and the action $\boldsymbol{\mathcal{S}}[X]$ is a functional of the random walk which in the continuum limit coincides with the time integral of the local energy:

$$\boldsymbol{\mathcal{S}}[X] = \epsilon\sum_{i=1}^{N}\mathcal{E}(x_i) + \mathcal{O}(\epsilon)$$

$$\approx \int_0^\tau \mathcal{E}(x(\tau'))d\tau'. \tag{48}$$

Eq. (47) is a generalization of the Feynman-Kac formula [12] and can be demonstrated as follows.

$$\mathcal{Z}_0 = \int \Phi_0(x)G(x,y;\tau)\Phi_0(y)\;dxdy, \tag{49}$$

where

$$G(x,y;\tau) = \langle x|\mathrm{e}^{-H\tau}|y\rangle \tag{50}$$

is the imaginary-time propagator of the full Hamiltonian. We now break the propagator in Eq. (49) into the product of N short-time propagators:

$$\mathcal{Z}_0 = \int \underbrace{\Phi_0(x_0)G(x_0,x_1;\epsilon)\cdots G(x_{N-1},x_N;\epsilon)\Phi_0(x_N)}_{\mathbf{P}[X]}\;\boldsymbol{\mathcal{D}}[X]. \tag{51}$$

Eqs. (47) and (51) can be seen as a *definition* of the action:

$$\mathbf{P}[X] = \boldsymbol{\mathcal{P}}[X]\mathrm{e}^{-\boldsymbol{\mathcal{S}}[X]}. \tag{52}$$

By using the Trotter formula,

$$G(x, y; \epsilon) = \mathcal{G}(x, y; \epsilon)\mathrm{e}^{-\epsilon\ \mathcal{E}(y)} + \mathcal{O}\left(\epsilon^2\right), \tag{53}$$

one sees that the action defined by Eq. (52) can indeed be expressed by the time integral given by Eq. (48).

$\mathcal{Z}_0$ plays the role of a pseudo partition function, in the sense that the energy of the system—as well as other observables, as we will see—can be calculated by differentiating it much in the same way as one would do in classical statistical mechanics. In particular, the two expression (44) and (45) for the ground-state energy correspond to the zero-temperature limits of the internal and free energies, respectively. By inserting Eq. (47) into Eq. (45), one could derive a systematic perturbative expansion of the ground-state energy in powers of $\mathcal{E}(x) - \bar{\mathcal{E}}$. Each term of the series is basically a cumulant of the action, which in turn can be seen as the integral of a suitably defined *connected* time correlation function of the local energy, calculated along the Langevin random walk. This kind of *stochastic* perturbation theory can be effectively carried on to infinite order by inserting Eq. (47) into Eq. (44). The final result reads:

$$\begin{aligned} E_0 &= \lim_{\tau\to\infty} \frac{\left\langle \mathcal{E}(x(\tau))\mathrm{e}^{-\boldsymbol{\mathcal{S}}[X]} \right\rangle}{\left\langle \mathrm{e}^{-\boldsymbol{\mathcal{S}}[X]} \right\rangle} \\ &\equiv \lim_{\tau\to\infty} \langle\!\langle \mathcal{E}(x(\tau)) \rangle\!\rangle , \end{aligned} \tag{54}$$

where the double bracket $\langle\!\langle\cdot\rangle\!\rangle$ indicates that the average over the random walks (*quantum paths*) is re-weighted by the exponential of the action, Eq. (48).

Eq. (54) can be turned into an algorithm for calculating the ground-state energy. The calculation would proceed as in a standard VMC simulation, with the difference that the local energy must be weighted with the exponential of the action, $\mathrm{e}^{-\boldsymbol{\mathcal{S}}}$, calculated along a segment of the random walk of length τ and ending at the time when the measure is taken. This algorithm, which was first proposed in Ref. [4], is bound to fail in all those case where the number of particles is so large or the quality of the trial wavefunction is so poor that the fluctuations of the action make the weighting procedure impractical. As a matter of fact, the *pure-diffusion Monte Carlo* (PDMC) of Ref. [4] has only been applied to very simple quantum systems. In the next session we will show how the fluctuations of the action can be effectively dealt with through a new algorithm based on importance sampling. Before doing this, we want to show how the ideas exposed so far can be exploited to calculate general ground-state expectation values and response functions.

3.2. CALCULATION OF OBSERVABLES

Other local observables can be calculated along similar lines starting from the Hellman-Feynman theorem [13]:

$$\langle \Psi_0 | \mathcal{A} | \Psi_0 \rangle = \left. \frac{dE_\lambda}{d\lambda} \right|_{\lambda=0}, \tag{55}$$

where E_λ is the ground-state energy of a system whose Hamiltonian is

$$H_\lambda = H + \lambda \mathcal{A}. \tag{56}$$

By using Eq. (45), E_λ can be put in the form:

$$E_\lambda = -\lim_{\tau\to\infty} \frac{1}{\tau} \log \left\langle \mathrm{e}^{-\boldsymbol{\mathcal{S}}_\lambda[X]} \right\rangle, \tag{57}$$

where

$$\boldsymbol{\mathcal{S}}_\lambda[X] = \int_0^\tau \left(\mathcal{E}(x(\tau')) + \lambda \mathcal{A}(x(\tau')) \right) d\tau'. \tag{58}$$

The expectation value of $\mathcal{A}$ can then be expressed as:

$$\begin{aligned} \langle \Psi_0 | \mathcal{A} | \Psi_0 \rangle &= \lim_{\tau\to\infty} \frac{\left\langle \frac{1}{\tau} \int_0^\tau \mathcal{A}(x(\tau')) d\tau' \mathrm{e}^{-\int_0^\tau \mathcal{E}(\tau') d\tau'} \right\rangle}{\left\langle \mathrm{e}^{-\int_0^\tau \mathcal{E}(\tau') d\tau'} \right\rangle} \\ &\equiv \lim_{\tau\to\infty} \left\langle\!\!\left\langle \frac{1}{\tau} \int_0^\tau \mathcal{A}(x(\tau'))\, d\tau' \right\rangle\!\!\right\rangle \end{aligned} \tag{59}$$

3.3. RESPONSE FUNCTIONS

A simple extension of the ideas used in the previous section leads to a technique for evaluating response functions. Let us suppose that the system is coupled to a set of external variables, $\{\lambda_i\}$, through the local operators $\{\mathcal{A}_i\}$:

$$H_{\{\lambda\}} = H + \sum_i \lambda_i \mathcal{A}_i. \tag{60}$$

In the case of an external potential, for instance, the index i labels the coordinate, x, λ_i is the potential itself, $V_{ext}(x)$, and $\mathcal{A}_i$ is the particle-density operator, $n(x)$. We define a generalized susceptibility, χ, as the derivative of the expectation value of one of the $\mathcal{A}$ operators with respect to one of the λ's:

$$\begin{aligned}\chi_{ij} &= \frac{\partial\langle\mathcal{A}_i\rangle}{\partial\lambda_j} \\ &= \frac{\partial^2 E_\lambda}{\partial\lambda_i\partial\lambda_j}.\end{aligned} \tag{61}$$

By using Eq. (57), χ can be put in the form:

$$\begin{aligned}\chi_{ij} &= -\lim_{\tau\to\infty}\frac{1}{\tau}\left[\left\langle\!\!\left\langle\left(\int_0^\tau \mathcal{A}_i(\tau')d\tau'\int_0^\tau \mathcal{A}_j(\tau')d\tau'\right)\right\rangle\!\!\right\rangle\right. \\ &\qquad\qquad\left. -\left\langle\!\!\left\langle\int_0^\tau \mathcal{A}(\tau')d\tau'\right\rangle\!\!\right\rangle^2\right] \\ &= -\lim_{\tau\to\infty}\frac{1}{\tau}\left\langle\!\!\left\langle\int_0^\tau d\tau_1\int_0^\tau d\tau_2\left(\mathcal{A}_i(\tau_1)\mathcal{A}_j(\tau_2)-\bar{\mathcal{A}}_i\,\bar{\mathcal{A}}_j\right)\right\rangle\!\!\right\rangle,\end{aligned} \tag{62}$$

where $\bar{\mathcal{A}}$ is the time average of $\mathcal{A}$ over the random walk: $\bar{\mathcal{A}} = \frac{1}{\tau}\int_0^\tau \mathcal{A}(\tau')d\tau'$. We now split the domain of integration $[0 \le \tau_1 \le \tau; 0 \le \tau_2 \le \tau]$ into two sub-domains $[\tau_1 < \tau_2]$ and $[\tau_2 < \tau_1]$, and change the variables of integration $\{\tau_1,\tau_2\} \to \{\tau_1,\tau_2-\tau_1\}$ and $\{\tau_1,\tau_2\} \to \{\tau_1-\tau_2,\tau_2\}$ in the two sub-domains respectively. In the large τ limit, the susceptibility can then be cast into the form:

$$\chi_{ij} = -\left\langle\!\!\left\langle\int_0^\tau [c_{ij}(\tau')+c_{ji}(\tau')]d\tau'\right\rangle\!\!\right\rangle, \tag{63}$$

where the time auto-correlation function is defined by:

$$c_{ij}(\tau) = \frac{1}{\tau}\int_0^\tau \mathcal{A}_i(\tau')\mathcal{A}_j(\tau')d\tau' - \frac{1}{\tau^2}\int_0^\tau \mathcal{A}_i(\tau')d\tau'\int_0^\tau \mathcal{A}_j(\tau')d\tau'. \tag{64}$$

The symmetrized time correlation function $c_{ij}+c_{ji}$ is a functional of the path, whose time integral (*i.e.* whose $\omega = 0$ Fourier component) provides an estimator for the static response function. This argument can be easily generalized to show that other ($\omega \ne 0$) Fourier components of the same time correlation function provide suitable estimators for the dynamic susceptibility.

4. The algorithm

In the previous section we have shown that the calculation of ground-state expectation values and response functions can be reduced to the weighted average of suitable estimators over the space of random walks. A straightforward evaluation of these averages over a Langevin trajectory would be very inefficient because the weight, $e^{-\boldsymbol{\mathcal{S}}}$, may vary a lot. This problem can be solved by converting the *weighting* of the quantum paths into a *re-sampling* of them, through an appropriate Metropolis algorithm [14]. As a by-product, the use of the Metropolis algorithm allows one to reduce the systematic errors due to the discretization of time in an efficient and convenient way.

Let $G^{(n)}$ be any approximation to the full imaginary-time propagator, Eq. (50), correct to order n in ϵ, and $\mathbf{P}^{(n)}[X]$ the corresponding approximation to $\mathbf{P}[X]$, Eq. (51), which will be affected by errors of order n. Let us also define the corresponding approximations for the unperturbed propagator, $\mathcal{G}^{(n)}$, Eq. (24), path probability distribution, $\boldsymbol{\mathcal{P}}^{(n)}$, and time-discretization correction factor, $\boldsymbol{\mathcal{Q}}_\epsilon^{(n)}$, Eq. (25), and action, $\boldsymbol{\mathcal{S}}^{(n)}[X]$, Eq. (52). For instance, one can take:

$$
\begin{aligned}
G^{(2)}(x,y;\epsilon) &= \frac{1}{\sqrt{4\pi\epsilon}} e^{-\frac{(x-y)^2}{4\epsilon}-\frac{\epsilon}{2}(V(x)+V(y))} = G(x,y;\epsilon)+\mathcal{O}\left(\epsilon^3\right), \\
\mathcal{G}^{(2)}(x,y;\epsilon) &= \frac{1}{\sqrt{4\pi\epsilon}} e^{-\frac{(x-y)^2}{4\epsilon}-\frac{\epsilon}{2}\left(\frac{\Phi_0''(x)}{\Phi_0(x)}+\frac{\Phi_0''(y)}{\Phi_0(y)}\right)} = \mathcal{G}(x,y;\epsilon)+\mathcal{O}\left(\epsilon^3\right), \\
\boldsymbol{\mathcal{P}}^{(2)}[X] &= \Phi_0(x_N)\mathcal{G}^{(2)}(x_N,x_{N-1};\epsilon)\cdots\mathcal{G}^{(2)}(x_1,x_0;\epsilon)\Phi_0(x_0) \\
&= \boldsymbol{\mathcal{P}}[X]+\mathcal{O}\left(\epsilon^2\right), \qquad (65) \\
\boldsymbol{\mathcal{S}}^{(2)}[X] &= e^{-\frac{\epsilon}{2}\sum_{i=1}^N(\mathcal{E}(x_i)+\mathcal{E}(x_{i-1}))} = \boldsymbol{\mathcal{S}}[X]+\mathcal{O}\left(\epsilon^2\right).
\end{aligned}
$$

Any ground-state expectation value or response function can be put in the form:

$$\langle\!\langle \mathbf{F}[X] \rangle\!\rangle = \frac{\int \mathbf{P}^{(n)}[X]\ \mathbf{F}[X]\ \boldsymbol{\mathcal{D}}[X]}{\int \mathbf{P}^{(n)}[X]\ \boldsymbol{\mathcal{D}}[X]} + \mathcal{O}\left(\epsilon^n\right). \qquad (66)$$

In order to calculate the above expectation value through the Metropolis method, it is necessary to construct a Markov chain of random walks so that the corresponding transition probability, $\mathbf{W}[Y \leftarrow X]$, satisfies detailed balance:

$$\mathbf{W}[Y \leftarrow X] \times \mathbf{P}^{(n)}[X] = \mathbf{W}[X \leftarrow Y] \times \mathbf{P}^{(n)}[Y] \qquad (67)$$

In the Metropolis algorithm, the transition probability $\mathbf{W}$ is split into the product of an *a-priori* transition probability, $\mathbf{W}^0$, times a probability, $\mathbf{A}$, that a move *proposed* according to $\mathbf{W}^0$ is accepted: $\mathbf{W}[Y \leftarrow X] = \mathbf{W}^0[Y \leftarrow X] \times \mathbf{A}[Y \leftarrow X]$. Detailed balance, Eq. (67), can be satisfied by choosing [15]:

$$\mathbf{A}[Y \leftarrow X] = \min(1, \mathbf{R}[Y \leftarrow X]), \qquad (68)$$

where

$$\mathbf{R}[Y \leftarrow X] = \frac{\mathbf{W}^0[X \leftarrow Y] \times \mathbf{P}^{(n)}[Y]}{\mathbf{W}^0[Y \leftarrow X] \times \mathbf{P}^{(n)}[X]}. \qquad (69)$$

Given a quantum path, $X \equiv \{x_0, \cdots, x_N\}$, we propose a new path, Y, by propagating the random walk forward by $M < N$ steps, according to the VMC Langevin equation, Eqs. (2,37): $Y \equiv \{x_M, \cdots, x_N, \cdots, x_{M+N}\}$. The corresponding a-priori transition probability is:

$$\begin{aligned} \mathbf{W}^0[Y \leftarrow X] &= \mathcal{W}_\epsilon(x_{N+M}|x_{N+M-1}) \cdots \mathcal{W}_\epsilon(x_{N+1}|x_N) \\ &= \boldsymbol{\mathcal{P}}^{(n)}[\{x_N, \cdots, x_{N+M}\}] \boldsymbol{\mathcal{Q}}_\epsilon^{(n)}[\{x_N, \cdots, x_{N+M}\}]/P_s(x_N), \end{aligned} \tag{70}$$

where we have used Eq. (25). By inserting this expression for the a-priori probability into Eq. (69), the latter can be cast into the form:

$$\begin{aligned} \mathbf{R}[Y \leftarrow X] = & \frac{\boldsymbol{\mathcal{P}}^{(n)}[\{x_M, \cdots, x_0\}] \times \boldsymbol{\mathcal{Q}}_\epsilon^{(n)}[\{x_M, \cdots, x_0\}]/P_s(x_M)}{\boldsymbol{\mathcal{P}}^{(n)}[\{x_N, \cdots, x_{N+M}\}] \times \boldsymbol{\mathcal{Q}}_\epsilon^{(n)}[\{x_N, \cdots, x_{N+M}\}]/P_s(x_N)} \\ & \times \boldsymbol{\mathcal{P}}^{(n)}[\{x_0, \cdots, x_N\}] \times \frac{\mathrm{e}^{-\boldsymbol{\mathcal{S}}^{(n)}[X]}}{\boldsymbol{\mathcal{P}}^{(n)}[\{x_M, \cdots, x_{N+M}\}] \times \mathrm{e}^{-\boldsymbol{\mathcal{S}}^{(n)}[Y]}}. \end{aligned} \tag{71}$$

With the aid of the composition law for the random-walk probability distributions, Eq. (26), and of the time–reversal property, Eq. (27), the above equation finally reads:

$$\mathbf{R}[Y \leftarrow X] = \mathrm{e}^{-(\boldsymbol{\mathcal{S}}^{(n)}[Y] - \boldsymbol{\mathcal{S}}^{(n)}[X])} \times \frac{\boldsymbol{\mathcal{Q}}_\epsilon^{(n)}[\{x_M, \cdots, x_0\}]}{\boldsymbol{\mathcal{Q}}_\epsilon^{(n)}[\{x_N, \cdots, x_{N+M}\}]}. \tag{72}$$

Notice that the ratio of the $\boldsymbol{\mathcal{Q}}$'s goes to one in the continuous-time limit ($\epsilon \to 0$) and that for finite ϵ it can be explicitly calculated, providing thus a systematic way for reducing to any desired order the time-discretization errors.

The dynamical variables of our simulations are quantum paths, which can be formally associated with polymers, much in the same spirit as this is done in path-integral simulations. The polymer dynamics which would correspond to our algorithm is known in the literature as *reptation* [16]. For this reason, we name our algorithm *Reptation Quantum Monte Carlo* (RQMC), and we refer to each individual quantum path as to a *reptile*.

The practical implementation of RQMC is extremely simple, at the level of a VMC simulation. The algorithm can be summarized as follows:

1. Using Eqs. (2) and (37), generate a reptile long enough that its end point, $x(T)$, is distributed according to the square of the trial wave function, Φ_0^2.
2. Generate a further segment of the reptile corresponding to the time interval $[T, T+\tau]$. $\tau = N\epsilon$ should be large enough that the limit $\tau \to \infty$ in Eqs. (54), (59), and (62) is reached to the desired accuracy. Set $X \equiv \{x_0, x_1, \cdots, x_N\} \leftarrow \{x(T), x(T+\epsilon), \cdots, x(T+\tau)\}$.

3. Select a 'direction of time' (*forward* or *backward*) with equal probability. If the choice is *backward*, set $X \leftarrow \bar{X} = \{x_N, x_{N-1}, \cdots, x_0\}$. This step is necessary to ensure the micro-reversibility of the algorithm.
4. Generate a segment of the reptile corresponding to the time interval $[T+\tau, T+\tau+\delta]$ and set $Y \equiv \{x_M, x_{M+1}, \cdots, x_{N+M}\} \leftarrow \{x(\delta), x(T+\delta+\epsilon), \cdots, x(T+\tau+\delta)\}$. The value of δ is sampled from an uniform deviate in the interval $[0, \Delta]$ whose width is chosen so as to minimize the auto-correlation times of the measured quantities. Sampling δ instead of keeping it constant helps to avoid that the reptile occasionally remains stuck at a fixed position for a long time.
5. Evaluate $\mathbf{R}[Y \leftarrow X]$ according to Eq. (72).
6. If $\mathbf{R} > 1$, set $X \leftarrow Y$. If $\mathbf{R} < 1$, set $X \leftarrow Y$ with probability $\mathbf{R}$.
7. Accumulate the ground-state energy and other observables using appropriate estimators (see the next section for an optimal choice of the estimators).
8. Go to 3.

A preliminary test of this algorithm has been performed for the hydrogen atom using an approximate trial function. Exact results for the average of several moments of electron–nucleus distance have been reproduced within a statistical error pushed down to a small fraction of the difference between the exact value and the extrapolated estimate (i.e. twice the mixed average minus the variational average [17]).

5. A case study of ^{4}He

We now discuss the calculation of several properties of superfluid ^{4}He, with the purpose of showing that the method can be successfully applied to systems of actual physical interest. Based on the limited experience gained in this case study, we also present some performance comparisons with related techniques.

5.1. DETAILS OF THE SIMULATION

We consider $N_P = 64$ ^{4}He atoms interacting through a pair potential, as obtained from first-principles calculations [18]. The simulation was performed in a cubic box with periodic boundary conditions at the experimental equilibrium density, $\rho = 0.02186$ Å^{-3}. The trial function Φ_0 includes pair and nearly optimal three–body correlations [19]. This is a relatively good trial function. The variational energy is less than 0.3 K above the exact ground-state energy, whereas the variational bias is larger than 1.1 K using pair correlations only. The quantities we compute are total and potential energies, the imaginary-time correlations of the density fluctuation operators,

$\rho_q = \sum_i \exp(-i\mathbf{q}\cdot\mathbf{r}_i)$:

$$F(q,\tau) = \langle \rho_q(\tau)\rho_q^\dagger(0)\rangle / N_P, \tag{73}$$

and the diffusion coefficient of the center of mass motion,

$$D(\tau) = \langle [\mathbf{r}_{CM}(\tau) - \mathbf{r}_{CM}(0)]^2 \rangle N_P/(6\tau). \tag{74}$$

The parameters of our simulations are as follows. The time step is $\epsilon = 0.001\ \mathrm{K}^{-1}$, which gives a systematic bias of the order of 10^{-2} K on the total energy. For the calculation of total and potential energy the length of the path was $\tau = 0.4\ \mathrm{K}^{-1}$, corresponding to $N = 400$ time slices. The calculation of imaginary-time correlations over a significant range required the use of longer paths, up to $N = 700$. The value of the energy resulting from the simulation with such longer paths confirmed that the finite-τ bias in the results obtained with $N = 400$ was smaller than statistical errors. Note that the length of the path adversely affects the efficiency, because the relaxation time of the polymer in the reptation algorithm is proportional to N^2 [20]. The number of time slices of each reptation move is uniformly sampled between 0 and 20, yielding an acceptance ratio of $\approx 80\%$.

Fluctuations in the average of the total energy are reduced using a symmetrized form of Eq. (54), *i.e.* accumulating $[\mathcal{E}(x(\tau)) + \mathcal{E}(x(0))]/2$. Expectation values of local observables are computed averaging time integrals along the path, Eq. (59) and Eq. (62). Although these expressions are exact in the $\tau \to \infty$ limit, the contributions coming from the extrema of the path are clearly biased. For instance, the average of $\mathcal{A}$ in the initial or final time slices ($\langle \mathcal{A}(x(0))\rangle$ and $\langle \mathcal{A}(x(\tau))\rangle$) yields the mixed estimate:

$$\lim_{\tau\to\infty} \frac{\left\langle \mathcal{A}(x(0))\mathrm{e}^{-\int_0^\tau \mathcal{E}(\tau')d\tau'}\right\rangle}{\left\langle \mathrm{e}^{-\int_0^\tau \mathcal{E}(\tau')d\tau'}\right\rangle} = \lim_{\tau\to\infty} \frac{\langle \Phi_0|\mathcal{A}\mathrm{e}^{-H\tau}|\Phi_0\rangle}{\langle \Phi_0|\mathrm{e}^{-H\tau}|\Phi_0\rangle} = \frac{\langle \Phi_0|\mathcal{A}|\Psi_0\rangle}{\langle \Phi_0|\mathcal{A}|\Psi_0\rangle}. \tag{75}$$

On the other hand any time slice a distance $\bar{\tau}$ apart from the extrema, such that $\exp(-H\bar{\tau})|\Phi_0\rangle \simeq |\Psi_0\rangle$, gives an unbiased contribution to the time integral of $\mathcal{A}$. Therefore it is convenient to restrict the time integral of $\mathcal{A}$ in Eqs. (59) and (62), to the inner section of the path, where the bias is reduced. For the potential energy and the imaginary-time correlations we exclude the contributions from 150 time slices on each side of the path. This is a rough estimate of the time it takes for the average potential energy to converge within a few hundredths K from its value at slice 0 or N_τ (which is by Eq. (75) the mixed estimate) to the unbiased estimate. This is demonstrated by the average of the potential energy on individual time

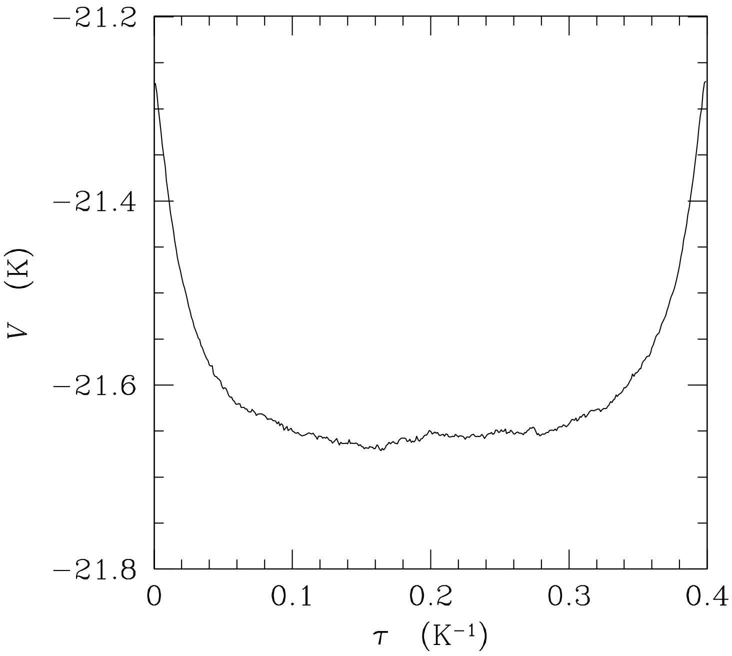

Figure 1. Average of the potential energy in ^{4}He, calculated on individual time slices along the path. The statistical error on the central slices is $\simeq 0.03$ K. This result was obtained using a trial function with pair correlations only: note that V converges to the same value given in Table 1, obtained using a trial function with pair and triplet correlations.

slices, shown in Fig. 1. We have not studied the corresponding convergence times for the density–density correlations.

5.2. RESULTS

Our results for the total and potential energies are listed in Table 1. The inter-particle potential adopted [18] overestimates the experimental binding energy of -7.17 K because of the neglect of three–body forces (mostly triple–dipole repulsion). Also reported in Table 1 are the corresponding

TABLE 1. Ground-state energy, E_0, and potential energy, V, in ^{4}He, as computed from RQMC and traditional diffusion Monte Carlo runs of 3×10^6 Monte Carlo steps. Units are K. The length of the path in the RQMC calculation is $\tau = 0.4$ K^{-1}, and the length of the forward walk for V in the diffusion Monte Carlo calculation is 0.2 K^{-1}.

	E_0	V
RQMC	-7.4066(27)	-21.644(15)
BDMC	-7.3902(15)	-21.674(21)

data obtained from a standard Branching Diffusion Monte Carlo (BDMC) calculation using the same time step and trial function. The small differences between the results of the two algorithms have to be attributed to different time-step biases.

In Fig. 2 we show the density-density correlation function, $F(q,\tau)$, for a few values of q, as obtained from a run of 10^7 MC steps, which required about one week CPU time on a workstation. Note that at virtually no additional cost many more q vectors, belonging to the reciprocal lattice of the simulation box, could have been included in the calculation.

$F(q,\tau)$ is related to several quantities of physical interest [21], including the static structure factor,

$$S(q) = F(q,0) = \int_0^\infty d\omega\ S(q,\omega), \tag{76}$$

the static linear response function,

$$\chi(q) = -2\int_0^\infty d\tau\ F(q,\tau) = -2\int_0^\infty d\omega\ S(q,\omega)/\omega, \tag{77}$$

and the dynamical structure factor,

$$F(q,\tau) = \int_0^\infty d\omega\ \mathrm{e}^{-\omega\tau}\ S(q,\omega). \tag{78}$$

Low moments of $S(q,\omega)$ can be accurately extracted from the simulation data for $F(q,\tau)$. The static structure factor, Fig. 3, and the static response, Fig. 4, compare very favorably with the experimental results, the discrepancy visible in $S(q)$ at the smallest value of q being due to the finite temperature at which the measurements are performed. The f–sum rule, $\partial F(q,\tau)/\partial\tau|_{\tau=0} = \int d\omega\ S(q,\omega)\omega = q^2$, is also verified with high precision.

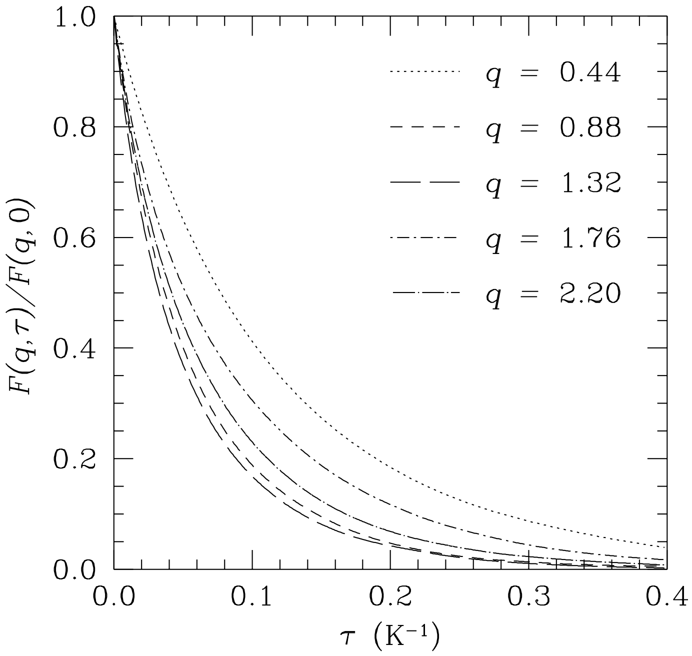

Figure 2. Imaginary-time correlations of the density fluctuation operator in ^{4}He. Averages are taken on the inner part of a path of length 0.7 K^{-1}. The statistical error ranges from approximately 0.5% at $\tau = 0$ up to 5% at $\tau = 0.4$ K^{-1}.

Inferring dynamical properties from imaginary-time correlations, on the other hand, is much harder. Since the inverse Laplace transform (78) with incomplete and noisy data for $F(q, \tau)$ is an ill–conditioned problem [24], a least χ^2 approach to pin down a parametrized form for $S(q, \omega)$ is doomed to failure. Additional constraints can be set on the solution $S(q, \omega)$ by resorting to Maximum Entropy (ME) methods [24]. We follow the implementation used in Ref. [25] to process data for $F(q, \tau)$ obtained at finite temperature with a PIMC simulation. The results are qualitatively similar to those obtained in Ref. [25]. The ME reconstruction of $S(q, \omega)$, shown in Fig. 5, is too smooth and does not reproduce the sharp features exhibited by the

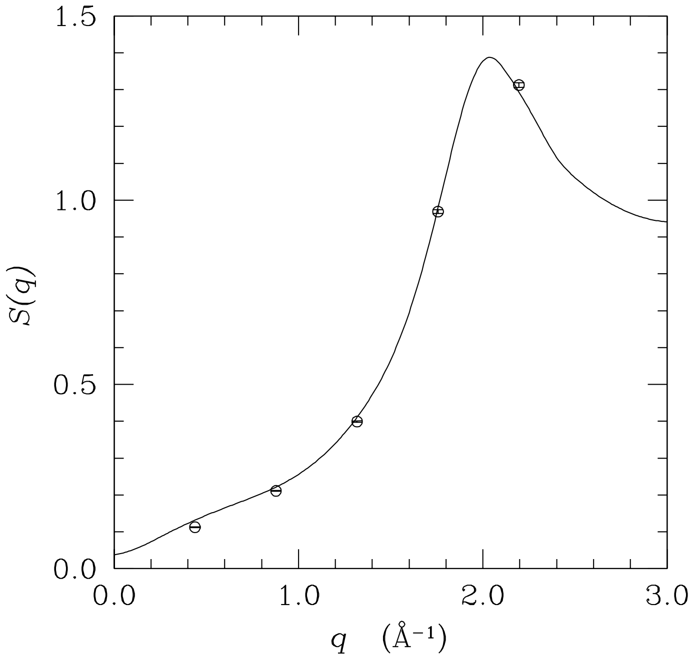

Figure 3. Static structure factor in ^{4}He at the five wave vectors listed in Fig. 2 (open circles). The solid line is the experimental $S(q)$ measured by neutron scattering [22].

experimental structure factor. Furthermore, the relatively poor quality of the available Monte Carlo data does not allow for a reliable estimate of the statistical uncertainty on the results [24]. Nevertheless we do recover some useful information on dynamical properties: the presence of a gap in the excitation spectrum is unambiguously revealed, and the position of the peak of the reconstructed dynamical response closely follows the experimental dispersion of the elementary excitations (see the inset of Fig. 5).

We now outline the calculation of the superfluid density ρ_s. Although the value of ρ_s/ρ is trivially one for pure bulk ^{4}He in the ground state, interacting Bose systems in the presence of an external disordered potential undergo a zero temperature superfluid–insulator transition as the strength

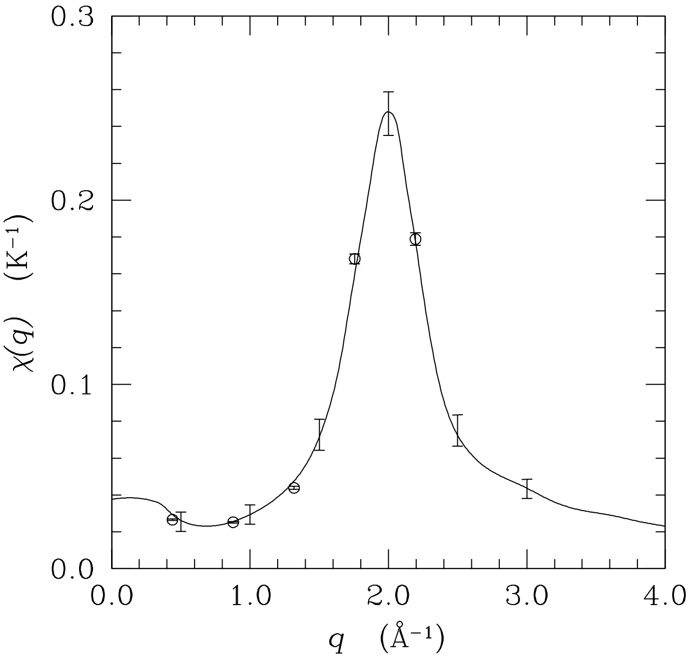

Figure 4. Static response function of ^{4}He at the five wave vectors listed in Fig. 2 (open circles). The solid line is the experimental result of Ref. [23].

of the potential increases [27]. We thus consider a model system of static impurities in ^{4}He. The external potential V_{ext} is represented by attractive Gaussians, $V_{ext}(\mathbf{r}) = \sum_j A \exp[-\alpha(\mathbf{r} - \mathbf{R}_j)^2]$, where the positions $\mathbf{R}_j$ of the impurities are placed randomly in the simulation box, $A = -50$ K and $\alpha = 0.5$ Å^{-2}. The trial function is multiplied by a one–body factor $\exp[-\sum_{i,j} f(|\mathbf{r}_i - \mathbf{R}_j|)]$ which tends to localize the ^{4}He atoms around the impurities. No average over different realizations of disorder was performed.

In a finite-temperature calculation with periodic boundary conditions, ρ_s can be estimated [28] as $\rho_s/\rho = \langle w^2 \rangle/(6\tau N_P)$, where the winding number $\mathbf{w} = \sum_{i=1}^{N_P} \int_0^\tau d\tau' \left[\frac{d\mathbf{r}_i(\tau')}{d\tau'}\right]$ is the displacement of the center of mass of the system, and τ is the inverse temperature. By taking the limit $\tau \to \infty$,

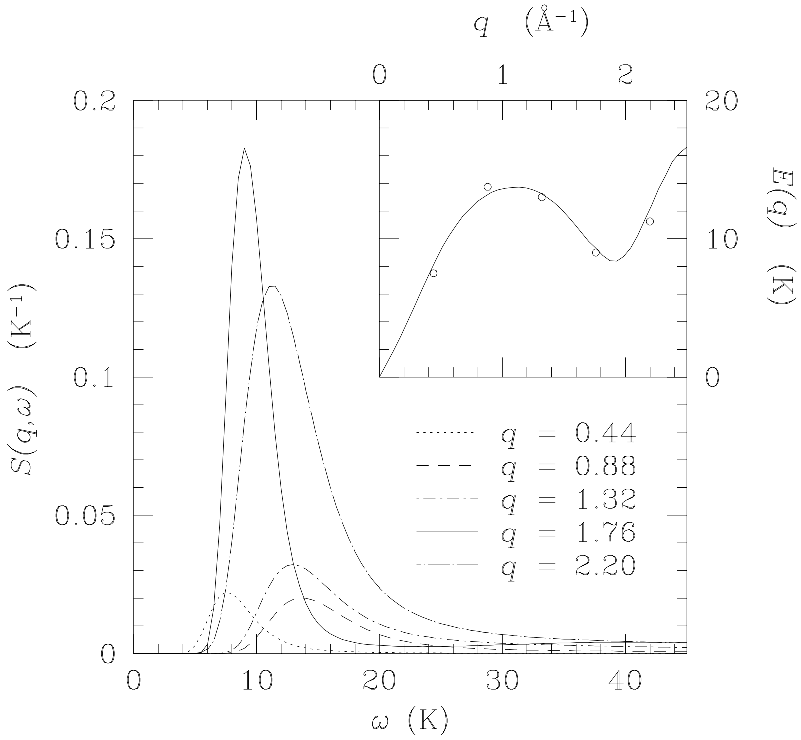

Figure 5. Maximum Entropy reconstruction of the dynamical structure factor of ^{4}He. In the inset the position of the maxima of the calculated $S(q, \omega)$ is compared with the experimental excitation spectrum [26].

appropriate for a ground-state calculation, the superfluid density at $T = 0$ can be expressed in terms of the diffusion coefficient of the center of mass motion, $\rho_s/\rho = \lim_{\tau\to\infty} D(\tau)$, where D is defined in Eq. (74).

The results reported in Fig. 6 show that the superfluid fraction, which is correctly one for the pure system, is indeed reduced in the presence of the impurities. Longer simulations would be needed to relate the depletion of the superfluid fraction induced by the disordered potential to changes of the excitation spectrum.

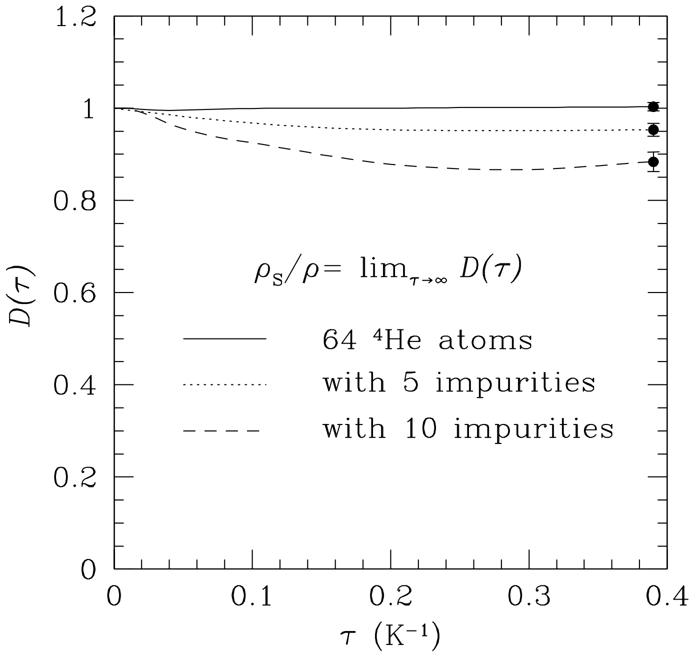

Figure 6. Diffusion coefficient of the center of mass motion of ^{4}He in the presence of quenched disorder.

5.3. COMPARISON WITH OTHER METHODS

Reptation quantum Monte Carlo utilizes the Metropolis algorithm to sample an explicitly known probability distribution, namely a discretized path integral expansion of $\exp(-\tau H)\Phi_0$ which becomes exact in the limit $\tau \to \infty$ and $\epsilon \to 0$. Sampling a distribution, as opposed to carrying weights, avoids the difficulties associated with fluctuating weights which plague applications of 'pure diffusion' [4] or 'single thread' [29] Monte Carlo. For instance, we were unable to get converged results for our 64 particle system with using pure-diffusion Monte Carlo [4].

The idea of sampling a path-integral representation of the imaginary-time evolution to compute ground-state properties is not new [30]. For instance, Variational Path Integral (VPI) [28] uses the pair product approximation to expand the many–body density matrix $\exp(-\tau H)$ and the bisection method to sample the path, just like in the usual Path Integral Monte Carlo method [28].

Reptation quantum Monte Carlo features instead an expansion of the imaginary-time propagator based on the Langevin dynamics generated by the trial function, and a reptation algorithm to sample the exponential of the resulting action. From the computational point of view, the advantage of this particular choice can be understood in the limit of perfect importance sampling: if the trial function is exact the local energy is a constant, and reptation moves consisting of an arbitrary number of time slices will be accepted with probability 1. Eventually, a very poor wave function (or equivalently a very large number of particles) will force us to take extremely small reptation moves, and moves of the kind used in VPI will become more efficient [28]. variational path integral has been implemented [31] for the simulation of superfluid ^{4}He at $T = 0$. According to the author of the VPI calculation, for the system size considered here RQMC is considerably more efficient.

Sampling an explicitly known distribution is to be contrasted to the standard branching diffusion Monte Carlo, which samples an unknown distribution (*i.e.* the mixed distribution $\Psi_0\Phi_0$) obtained from the asymptotic solution of a differential equation [32, 33]. BDMC is designed to compute efficiently the total energy; however it introduces a population-control bias, yields a mixed estimate for operators not commuting with H, and does not retain direct information on the imaginary-time correlations. This information can be retrieved through the 'forward walking' technique [33, 34] and used to correct both the population control and the mixed estimate biases, but at the price of additional statistical fluctuations. We believe that reptation quantum Monte Carlo will turn out to be advantageous over branching diffusion Monte Carlo in those cases where recovering information from fluctuating weights becomes too noisy.

The results for the total energy shown in Table 1 are obtained from reptation quantum Monte Carlo and branching diffusion Monte Carlo using the same time step, number of particles, and trial function. From the estimated statistical error we infer that BDMC is roughly 3 times faster than RQMC for the calculation of the total energy. Also listed in Table 1 are the unbiased estimates for the potential energy. In this case branching diffusion Monte Carlo with forward walking (implemented in the "backward storing mode" described in Ref. [33]) turns out to be roughly two times slower than reptation quantum Monte Carlo. Obviously, factors 2 or 3 for a couple of observables in a particular physical system are not a conclusive assessment of the relative performance of two algorithms. However the resulting factor 6 in the relative improvement of RQMC when BDMC has to be complemented with forward walking suggests that, whenever explicit information on imaginary-time correlations is used, reptation quantum Monte Carlo is likely to be competitive or better.

6. Conclusions

The most attractive feature of the reptation quantum Monte Carlo is that it uses the dynamical properties of the random walk in a way that is directly related to the imaginary-time properties of the physical system. A previous implementation of similar ideas [4] was based on re-weighting and the scope of its applications was severely restricted by the fluctuations of the weights. We have shown that, by simply complementing the method of Ref. [4] with a re-sampling of the paths based on the value of the action, the resulting RQMC algorithm can afford system sizes typical of current branching diffusion Monte Carlo simulations of continuous strongly interacting systems. Unbiased estimates, static responses and some insight into dynamical properties can be readily obtained. The dependence of the computational effort on the number of particles and on the quality of the trial function remains to be investigated. Such an analysis will determine whether this method can be useful in more general situations than ^{4}He bulk liquid. Clusters, films and superfluids in restricted geometries are natural candidates for further applications.

For Fermion problems one has either to resort to the fixed-node approximation [32], or to cope with the sign problem [35]. In the former case, the dynamical information contained in the path is incorrect [4], but still the explicit knowledge of the weights along the path makes the algorithm free from the mixed distribution and the population control biases; furthermore it gives easy access to interesting quantities, such as a low–variance estimator of Born–Oppenheimer forces in electronic systems [36]. In the latter case the dynamics is correct, and can be used for example to get information on the ground and excited states from the imaginary-time evolution in the transient regime [37]; in similar cases however the real bottleneck will remain the sign problem.

Reptation quantum Monte Carlo, variational path integral [28], and the technique discussed in Ref. [30] sample explicit expressions of the imaginary-time propagator with the Metropolis algorithm to calculate zero temperature properties. We believe that these methods are very promising and deserve more attention than they have received so far. All these methods are based on the Metropolis algorithm: they enjoy therefore of a large freedom in the choice of the transition probability [38], which is probably not yet fully exploited.

Acknowledgements

We are indebted with Kevin Schmidt for useful discussions and for communicating to us unpublished details of his VPI calculations on ^{4}He. We are grateful to Matteo Calandra for lending himself to be the first reader of these lecture notes and to Peter Nightingale for his inspired and careful proof-reading. Thanks to their comments and suggestions, these notes are now considerably better than they were before.

References

*. Also with: *CECAM*, Centre Européen de Calcul Atomique et Moléculaire, Lyon, France. Electronic address: `baroni@sissa.it` .

†. Also with: *ICTP*, The Abdus Salam International Centre for Theoretical Physics, Trieste, Italy. Electronic address: `moroni@sissa.it` .

1. E. Nelson, Phys. Rev. **150**, 1079 (1966); F. Guerra and P. Ruggiero, Phys. Rev. Lett. **31**, 1022 (1973).
2. G. Parisi and Wu Yongshi, Sci. Sin. **24**, 483 (1981). See also: *Stochastic Quantization*, edited by P. H. Damgaard and H. Hüffel (World Scientific, Singapore, 1988).
3. See, *e.g.*: *Monte Carlo Methods in Quantum Problems*, edited by M. H. Kalos, NATO ASI series C v. 125 (Reidel, Dordrecht 1984); *Proceedings of the Conference on Frontiers of Quantum Monte Carlo, LANL, September 1985*, edited by J. E. Gubernatis, J. Stat. Phys. **43**, 729–1244 (1986); *Monte Carlo Methods in Theoretical Physics* edited by S. Caracciolo and A. Fabrocini, (ETS, Pisa 1991); *Quantum Monte Carlo Methods in Condensed Matter Physics*, edited by M. Suzuki, (World Scientific, Singapore 1993).
4. M. Caffarel and P. Claverie, J. Chem. Phys. **88**, 1088 (1988); *ibid.* p. 1100.
5. I. S. Gradshteyn and I. M. Ryzhik, *Table of Integrals, Series, and Products*, 5th ed. (Academic Press, San Diego, 1994), p. 382 # 3.462–4.
6. For a general textbook on the theory of stochatic processes and its application to the physical sciences, see *e.g.*: C. W. Gardiner, *Handbook of Stochastic Methods*, 2nd ed. (Springer-Verlag, Berlin, 1985). A nice collection of historically important papers is reprinted in: *Selected Papers on Noise and Stochastic Processes*, edited by N. Wax (Dover Publications, New York, 1954).
7. H. Haken, Z. Physik B **24**, 321 (1976).
8. R. P. Feynman and A. R. Hibbs, *Quantum Mechanics and Path Integrals* (McGraw Hill, New York 1965).
9. See *e.g.* L. D. Landau and E. M. Lifshitz, *Quantum Mechanics* 3rd ed. (Pergamon Press, Oxford, 1977), chapt. III; R. Courant and D. Hilbert, *Methods of Mathematical Physics* (Interscience Publishers, New York, 1953), vol. I, chapt. VI.
10. This statement is only valid if $v(x) < +\infty$ everywhere inside the domain of x.
11. P. J. Rossky, J. D. Doll, and H. L. Friedman, J. Chem. Phys. **69**, 4628 (1978); the reduction of time-discretization errors in the context of diffusion quantum Monte Carlo is discussed *e.g.* in: P. J. Reynolds, D. Ceperley, B. J. Alder, and W. A. Lester, J. Chem. Phys. **77** 5593 (1982) and in: C. J. Umrigar, M. P. Nightingale, and K. J. Runge, J. Chem. Phys. **99**, 2865 (1993).
12. M. D. Donsker and M. Kac, J. Res. Natl. Bur. Stand. **44**, 581 (1950); R. P. Feynman, *Statistical Mechanics* (Benjamin, Reading, MA, 1972).
13. H. Hellmann, *Einführung in die Quantenchemie* (Deuticke, Leipzig, 1937); R. P. Feynman, Phys. Rev. **56**, 340 (1939).

14. N. Metropolis, A. W. Rosenbluth, M. N. Rosenbluth, A. H. Teller, and E. Teller, J. Chem. Phys. **21**, 1087 (1953).
15. In the original Metropolis algorithm, the a-priori probability was actually assumed to be symmetric. A generalization to non-symmetric a-priori probabilities was apparently first discussed in: W. K. Hastings, Biometrika **57**, 97 (1970). See also: D. Ceperley, G. V. Chester, and M. H. Kalos, Phys. Rev. B **16**, 3081 (1977) and C. J. Umrigar, Phys. Rev. Lett. **71**, 408 (1993).
16. *Monte Carlo and Molecular Dynamics Simulations in Polymer Science*, edited by K. Binder, (Oxford University Press, 1995).
17. D. M. Ceperley and M. H. Kalos, in *Monte Carlo Methods in Statistical Physics*, edited by K. Binder (Springer-Verlag, 1979).
18. T. Korona, H. L. Williams, R. Bukowski, B. Jeziorski, and K. Szalewicz, J. Chem. Phys. **106**, 5109 (1997).
19. S. Moroni, S. Fantoni, and G. Senatore, Phys. Rev. B **52**, 13547 (1995).
20. I. Webman, J. L. Lebowitz, and M. H. Kalos, J. Physique **41**, 579 (1980).
21. D. Pines and P. Nozières, *Theory of Quantum Liquids* (Benjamin, 1966).
22. E. C. Svensson, V. F. Sears, A. D. B. Woods, and P. Martel, Phys. Rev. B **21**, 3638 (1980).
23. A. D. B. Woods and R. A. Cowley, Rep. Prog. Phys. **36**, 1135 (1973).
24. J. E. Gubernatis and M. Jarrell, Phys. Rep. **269**, 135 (1996).
25. M. Boninsegni and D. M. Ceperley, J. Low Temp. Phys. **104**, 339 (1996).
26. R. J. Donnelly, J. A. Donnelly, and R. N. Hills, J. Low Temp. Phys. **44**, 471 (1981).
27. M. P. A. Fisher, P. B. Weichman, G. Grinstein, and D. S. Fisher, Phys. Rev. B **40**, 546 (1989).
28. D. M. Ceperley, Rev. Mod. Phys. 67, 279 (1995).
29. M. P. Nightingale, in this volume, sec. III.
30. Ref. [29], sec. IV.
31. K. E. Schmidt, private communication.
32. L. Mitas, in this volume.
33. Ref. [29], sec. V.
34. K. S. Liu, M. H. Kalos, and G. V. Chester, Phys. Rev. A **10**, 303 (1974).
35. M. H. Kalos and F. Pederiva, in this volume.
36. F. Zong and D. M. Ceperley, submitted to Phys. Rev. E May 1998.
37. D. M. Ceperley and B. Bernu, J. Chem. Phys. **89**, 6316 (1988); B. Bernu, D. M. Ceperley, and W. A. Lester, J. Chem. Phys. **93**, 552 (1990). erratum **95**, 7782 (1991); M. Caffarel and D. M. Ceperley, J. Chem. Phys. **97**, 8415 (1992).
38. C. J. Umrigar, in this volume.